Direct growth of novel alloyed PtAu nanodendrites†

Jingpeng Wang,[ab] Dan F. Thomas[b] and Aicheng Chen*[a]

Received (in Cambridge, UK) 9th May 2008, Accepted 15th July 2008
First published as an Advance Article on the web 1st September 2008
DOI: 10.1039/b807660j

A novel nanostructure of a PtAu catalyst, alloyed PtAu nanodendrites, has been synthesized *via* a reproducible single-step hydrothermal co-reduction of Pt and Au inorganic precursors and shows exceptionally high catalytic activity towards the electrooxidation of formic acid.

The scientific roles of Au and Pt prepared in nanocrystalline forms have been extensively explored due to their distinctively different properties when compared to their bulk counterparts. Au, previously deemed catalytically less active than other noble metals, has attracted much attention recently with the development of nanocrystalline Au-based catalysts, showing higher catalytic properties for heterocatalysis and biosensing.[1] Pt-based nanomaterials have also been widely studied because of their impressive technological applications including fuel-cell technology, hydrogenation reaction, and the development of sensors and nanodevices.[2] Pt and Au, due to the miscibility gap in their binary phase diagram, are difficult to be prepared as homogeneous alloyed catalysts; phase segregation is expected. Consequently, the physical and chemical properties of PtAu alloys have largely not been unraveled. Recent studies have shown that monodispersed Pt–Au bimetallic and Pt–Au core–shell nanoparticles (NPs) can be formed.[3] However, the preparation of those Pt–Au NPs involves complicated and time-consuming synthetic routes and requires a large amount of organic compounds as solvents and/or surfactants. Thus, there is great interest in developing a facile and environment-friendly approach to synthesize PtAu nanostructures.

A dendrite has a main trunk with hierarchical side branches. On the nanoscale, dendritic fractals of several materials have been formed *via* hierarchical self-assembly under non-equilibrium conditions.[4] Nanodendrites, due to their higher structural complexity compared to nanoparticles, nanowires and nanospheres, are expected to have a wide range of technological applications, such as interconnections in the bottom-up self-assembly of nanocircuits and nanodevices.[5] However, the challenge is to develop simple and efficient synthetic approaches for building hierarchically self-assembled fractal architectures. In this communication, for the first time we report on a reproducible approach to synthesize large-scale alloyed PtAu nanodendrites *via* a facile single-step hydrothermal co-reduction of Pt and Au inorganic precursors. The as-synthesized PtAu nanodendrites with face centered cubic (fcc) alloy structure show exceptionally high activity towards the electrooxidation of formic acid.

To grow the alloyed PtAu nanodendrites, etched Ti plates were placed in a Teflon lined autoclave containing a 10 mL aqueous mixture of 5.0 mM H_2PtCl_6 + 5.0 mM $HAuCl_4$ + 1.0 M ammonium formate, with pH adjusted by formic acid to 5.5–6.5. The autoclave was sealed and heated at 180 °C for 8 h. After cooling to room temperature, the catalyst-coated Ti plates were annealed in a tube furnace at 250 °C under argon flow for 2 h, and then rinsed with pure water. Fig. 1(a) presents a typical scanning electron microscopic (SEM) image of the synthesized PtAu catalyst showing the formation of three-dimensional dense-branching nanostructures. The discernible cluster size is about 80–100 nm, and the length of the trunks varies from 1 to 10 μm.

Fig. 1(b) presents a typical transmission electron microscopic (TEM) image of a portion of a branch wherein densely packed grains of 7–10 nm can be identified as the building blocks of the clusters. The inter-connected grains possess no discernible difference in their morphology and size, indicating that each grain was formed as a monodispersed entity. Further energy dispersive X-ray spectroscopic (EDS) analysis and X-ray photoelectron spectroscopic (XPS) study showed that the composition of the formed PtAu nanodendrites, expressed in atomic ratio, is close to 1 : 1 (see Fig. S2 in ESI†). Fig. 1(c) presents a selected area electron diffraction (SAED) pattern

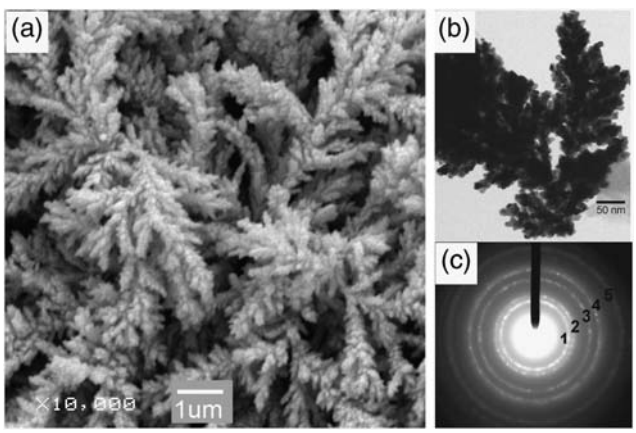

Fig. 1 SEM image (a) and TEM image (b) of the as-synthesized PtAu catalyst; SAED pattern (c) of the ramified branches shown in (b). (Additional TEM image of the synthesized dendritic PtAu is available in Fig. S1 in ESI†).

[a] *Department of Chemistry, Lakehead University, Thunder Bay, Ontario, Canada P7B 5E1. E-mail: aicheng.chen@lakeheadu.ca; Fax: 1-807-346-7775; Tel: 1-807-343-8318*
[b] *Department of Chemistry, University of Guelph, Guelph, Ontario, Canada N1G 2W1*

† Electronic supplementary information (ESI) available: Experimental details regarding the characterization methods; additional TEM image of synthesized PtAu nanodendrites; EDS and XPS spectra of PtAu alloy catalysts; chronoamperometry curves of selected electrodes in formic acid oxidation and a table listing all the steady-state current densities. See DOI: 10.1039/b807660j

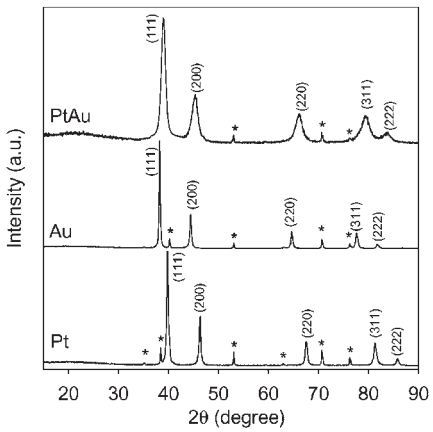

Fig. 2 XRD patterns recorded from the as-synthesized PtAu catalyst, Pt particles and Au particles. Peaks labelled by an asterisk are ascribed to the diffractions from the Ti substrate.

showing that the formed nanodendrites are polycrystalline. The as-labelled diffraction rings 1–5 correspond to (111), (200), (220), (311) and (222) reflections, respectively, all of which reveal the fcc crystal structure.

Fig. 2 presents the X-ray diffraction (XRD) patterns of the synthesized PtAu nanodendrites, together with two control samples: Pt NPs and Au NPs synthesized under the same hydrothermal method as that for PtAu nanodendrites. All peaks, in the spectra of pure Pt, pure Au and the PtAu alloy, except those from Ti substrate, can be indexed to fcc crystal structures. The alloyed nature of the synthesized PtAu dendrites can be inferred by the following evidence: (i) there are no distinct reflections characteristic of pure Pt and Au found in the PtAu XRD spectrum; (ii) the peak 2θ values of the PtAu diffraction patterns fall exactly between those of pure Pt and pure Au NPs; and (iii) the highly symmetric PtAu reflection peaks can be perfectly fitted with a single analytical function, suggesting that the as-synthesized PtAu catalyst is a single-phase nanomaterial, *i.e.* an alloy. The fcc lattice constant a of the synthesized PtAu nanodendrites, based on the 2θ values of the (220) peak, is calculated to be 0.399 nm, which is slightly higher than that of the synthesized Pt NPs (0.392 nm). By employing the Scherrer formula,[6] the average crystallite size of the PtAu dendrites is calculated to be 6–9 nm, in good agreement with the TEM results shown in Fig. 1(b).

To understand the formation mechanism of the alloyed PtAu dendrites, time-dependent experiments were carried out by quenching the Teflon-lined autoclave using cold water at different reaction stages. A series of SEM images and EDS spectra taken at different reaction times (t) are presented in Fig. 3. When t = 10 min, a gel-like coating layer on top of the substrate became visible, with aggregated small clusters embedded therein. At t = 30 min, the gel-like coating started developing into fishbone-like branched structures, which is considered as evidence for a prototype dendrite emerging from the gel-like solids. The formation of the highly ordered fish-bone-like morphology shows that, at this initial reaction stage, the nucleation and formation of dendrites are mainly dominated by oriented anisotropic growth along certain directions, rather than the diffusion-limited aggregation (DLA) of individual particles. This further indicates that the $HCOO^-$ ligand serves as not only a reducing agent, but also a capping agent that dictates the oriented growth direction. When t = 1 h, the gel-like coating layer became thicker, with many branched clusters mixed together. Dendritic PtAu structures became discernible at t = 2 h. During this stage, the fishbone-like morphology seen in Fig. 3(b) has developed into hyper-branched dendrites (dendritic fractals), indicating that the oriented growth of dendritic structure at this stage was surpassed by the DLA process. Subsequent nucleation and growth along the dendrite trunks and sub-trunks gave rise to secondary, tertiary and higher-order branches forming the dense-branching morphology shown in Fig. 3(e). It has been suggested that the fractal pattern is formed in situations far from thermodynamic equilibrium where high driving forces lead to the generation of rough crystallites and random association.[7] This may well explain the polycrystalline nature of the PtAu nano-dendrites formed in our study. The EDS analysis (Fig. 3(f)) reveals that the gel-like solid phase always contains Pt, Au and Cl with an atomic ratio close to 1 : 1 : x, where x varies from 1 to 2. The peak intensity of Cl is much lower than that of Au, Pt and Ti due to the fact that Cl is a fairly light element compared to Au, Pt and Ti. All the evidence indicates that a coordination–reduction mechanism may be involved in the formation of the alloyed phase of PtAu: the chlorine ligand in $PtCl_6^{2-}$ and $AuCl_4^-$ are first partially replaced by the $HCOO^-$ group, which further induces direct internal electron transfer from carbon atoms to Pt and Au cores; the partially reduced Pt and Au further exchange their Cl with $HCOO^-$ ligands and are reduced to

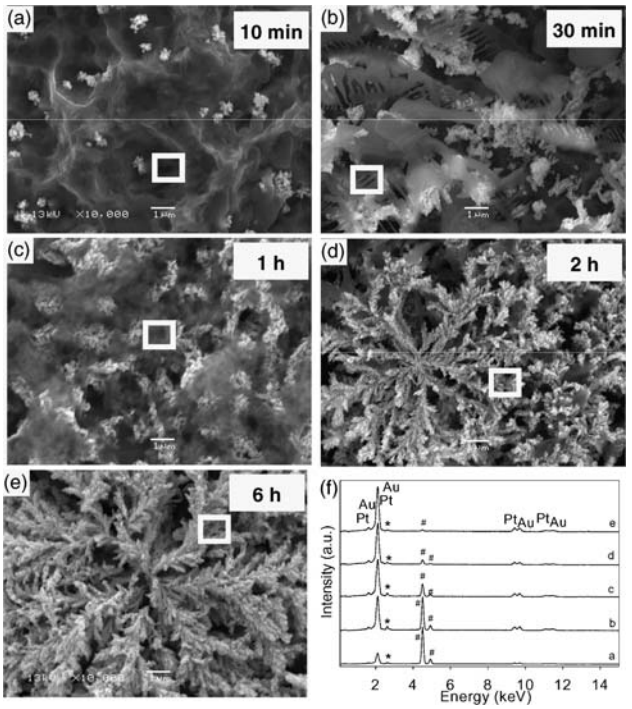

Fig. 3 (a)–(e) SEM images taken at different hydrothermal reaction times. (f) Corresponding EDS spectra to the spots indicated by the white squares on images (a)–(e); the peak labelled by an asterisk is ascribed to the Cl signal, and those peaks labelled # are attributed to the Ti substrate.

form a metastable intermediate [Pt–Cl–Au]; then, upon further complexation with the $HCOO^-$ group, the intermediates are completely reduced to form alloyed PtAu with a 1 : 1 atomic ratio. This is consistent with our EDS and XPS results.

We further studied the effect of temperature, pH and different reducing agents on the morphology and composition of the formed PtAu nanodendrites. The temperature of the hydrothermal process is critical, significantly affecting the phase property. Segregated phases (*i.e.* Pt NPs, Au NPs and PtAu dendrite-like structures) were produced at 100 °C and 150 °C; while PtAu (1 : 1) alloyed nanodendrites were formed at 180 °C as shown in Fig. 1. When the pH value of the starting solutions was lower and higher than the range of 5.5–6.5, the alloyed dendrite structures are not formed; instead, agglomerated bimetallic Pt–Au particles are produced. The variations on the type of reducing agents were also studied, showing that the most commonly used water-soluble reducing agents, such as formaldehyde, ethylene glycol, oxalic acid and glycine, do not fulfill the functions as that of $HCOO^-$ group.

The electrocatalytic activity of the as-synthesized PtAu nanodendrites was probed using the electrooxidation of formic acid. Fig. 4(a) compares the cyclic voltammograms of the dendritic PtAu electrode and Pt NPs in 0.1 M HCOOH + 0.1 M H_2SO_4 at a potential scan rate of 20 mV s^{-1}. Based on the well accepted dual-path mechanism of formic acid oxidation on Pt-based catalysts,[8] the low onset potential (−0.20 V) of formic acid oxidation and the significantly enhanced current density in the low potential region (0.05–0.45 V) suggest that the oxidation of formic acid on the alloyed PtAu nanodendrites proceeds mainly through the preferred dehydrogenation path (*i.e.* direct oxidation of formic acid to CO_2). In the case of the Pt NPs, the oxidation of formic acid has a late onset potential (0.03 V) and high peak potential (0.62 V), indicating that the oxidation of formic acid occurs mainly through the dehydration pathway with intermediate CO involved. As expected, the Au NPs exhibit low electro-catalytic activity towards the electro-oxidation of formic acid; thus they are not included in Fig. 4 for comparison. As seen from the chronoamperometric tests (Fig. 4(b) and Fig. S3 in the ESI†), the synthesized PtAu catalyst delivers current densities over four times higher than that of the Pt NPs at 0.15 V (see Table S1 in ESI†), demonstrating the enhanced electrocatalytic activity of the PtAu nanodendrites resulting from the altered reaction pathway.

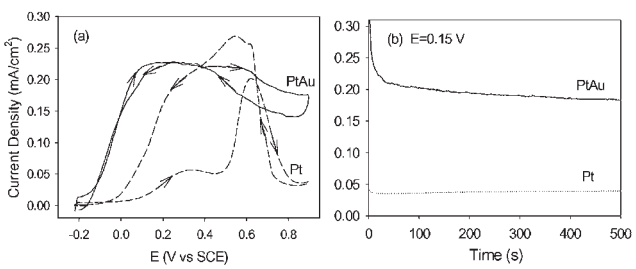

Fig. 4 Cyclic voltammograms at 20 mV s^{-1} (a) and chronoamperometric curve under 0.15 V (b) of the synthesized PtAu nanodendrites (solid line) and Pt nanoparticles (dashed line) in 0.1 M HCOOH + 0.1 M H_2SO_4. The current densities were calculated per active surface area of each electrode determined by hydrogen adsorption/desorption (see characterization methods in ESI†).

In summary, we have demonstrated a surfactant-free and environment-friendly approach to synthesize novel PtAu nanodendrites. The EDS, XPS, TEM, SAED and XRD characterizations have collectively confirmed that the formed PtAu nanodendrites are alloyed and close to 1 : 1 in atomic ratio. A coordination-reduction mechanism has been proposed to depict the hydrothermal reduction process. However, the question of how the oriented anisotropic growth and the diffusion-limited aggregation processes competed with each other and finally determined the hierarchical self-assembly at the microscopic scale remains unclear. To the best of our knowledge, the growth of fractal and dense-branching structures have never been reported on bimetallic Pt–Au systems, hence the simple system we reported herein would contribute to the further understanding of dendritic patterns' formation involving the DLA mechanism.[9] In addition, our electrochemical results have shown that the synthesized PtAu alloyed nanodendrites possess excellent electrocatalytic activity toward formic acid oxidation, promising for application in direct formic acid fuel cells.

This work was supported by a discovery grant from the Natural Sciences and Engineering Research Council of Canada (NSERC). A. Chen acknowledges the Canada Foundation of Innovation (CFI) and NSERC for the Canada Research Chair Award in Material and Environmental Chemistry.

Notes and references

1 (*a*) S. Lee, C. Fan, T. Wu and S. L. Anderson, *J. Am. Chem. Soc.*, 2004, **126**, 5682; (*b*) G. J. Hutchings, *Chem. Commun.*, 2008, 1148; (*c*) R. J. Stokes, A. Macaskill, J. A. Dougan, P. G. Hargreaves, H. M. Stanford, W. E. Smith, K. Fauldsa and D. Graham, *Chem. Commun.*, 2007, 2811.

2 (*a*) N. Tian, Z. Y. Zhou, S. G. Sun, Y. Ding and Z. L. Wang, *Science*, 2007, **316**, 732; (*b*) J. Wang, D. F. Thomas and A. Chen, *Anal. Chem.*, 2008, **80**, 997; (*c*) W. F. Paxton, P. T. Baker, T. R. Kline, Y. Wang, T. E. Mallouk and A. Sen, *J. Am. Chem. Soc.*, 2006, **128**, 14881; (*d*) C. Bock, C. Paquet, M. Couillard, G. A. Botton and B. R. MacDougall, *J. Am. Chem. Soc.*, 2004, **126**, 8028; (*e*) Y. Song, Y. Jiang, H. Wang, D. A. Pena, Y. Qiu, J. E. Miller and J. A. Shelnutt, *Nanotechnology*, 2006, **17**, 1300; (*f*) X. Peng, K. Koczkur, S. Nigro and A. Chen, *Chem. Commun.*, 2004, 2872.

3 (*a*) E. Bus and J. A. van Bokhoven, *J. Phys. Chem. C*, 2007, **111**, 9761; (*b*) H. Lang, S. Maldonado, K. J. Stevenson and B. D. Chandler, *J. Am. Chem. Soc.*, 2004, **126**, 12949; (*c*) J. Luo, M. M. Maye, V. Petkov, N. N. Kariuki, L. Wang, P. Njoki, D. Mott, Y. Lin and C.-J. Zhong, *Chem. Mater.*, 2005, **17**, 3086; (*d*) S. Zhou, K. McIlwrath, G. Jackson and B. Eichhorn, *J. Am. Chem. Soc.*, 2006, **128**, 1780; (*e*) L. Qian and X. Yang, *J. Phys. Chem. B*, 2006, **110**, 16672; (*f*) J. Xu, T. Zhao, Z. Liang and L. Zhu, *Chem. Mater.*, 2008, **20**, 1688.

4 (*a*) M. Cao, T. Liu, S. Gao, G. Sun, X. Wu, C. Hu and Z. L. Wang, *Angew. Chem., Int. Ed.*, 2005, **44**, 2; (*b*) Z. G. R. Tian, J. Liu, J. A. Voigt, H. F. Xu and M. J. Mcdermott, *Nano Lett.*, 2003, **3**, 89.

5 X. Teng and H. Yang, *Nano Lett.*, 2005, **5**, 885.

6 B. E. Warren, *X-ray Diffraction*, Dover Publications Inc., Mineola, NY, 1st edn, 1990.

7 (*a*) T. A. Witten, Jr and L. M. Sander, *Phys. Rev. Lett.*, 1981, **47**, 351; (*b*) P. Meakin, *Phys. Rev. Lett.*, 1983, **51**, 1119; (*c*) M. Wang, X. Y. Liu, C. S. Strom, P. Bennema, W. Enckevort and N. B. Ming, *Phys. Rev. Lett.*, 1998, **80**, 3089.

8 (*a*) N. M. Markovic, H. A. Gasteiger, P. N. Ross, X. Jiang, I. Villegas and M. J. Weaver, *Electrochim. Acta*, 1995, **40**, 91; (*b*) M. F. Mrozek, H. Luo and M. J. Weaver, *Langmuir*, 2000, **16**, 8463; (*c*) N. Kristian, Y. Yan and X. Wang, *Chem. Commun.*, 2008, 353.

9 (*a*) R. R. Brady and R. C. Ball, *Nature*, 1984, **309**, 225; (*b*) E. Ben-Jacob and P. Garik, *Nature*, 1990, **343**, 523; (*c*) V. Fleury, *Nature*, 1997, **390**, 145.

